ANALYSES OF ANNULAR LINEAR INDUCTION PUMP CHARACTERISTICS USING A TIME-HARMONIC FINITE DIFFERENCE ANALYSIS

SEUNG-HWAN SEONG* and SEONG-O KIM
Korea Atomic Energy Research Institute
P.O. Box 105 Yusong, Daejon 305-600, Korea
*Corresponding author. E-mail : shseong@kaeri.re.kr

Received November 29, 2007
Accepted for Publication January 23, 2008

The pumping of coolant in a liquid metal fast reactor may be performed with an annular linear induction electro-magnetic (EM) pump. Linear induction pumps use a traveling magnetic field wave created by poly-phase currents, and the induced currents and their associated magnetic field generate a Lorentz force, whose effect can be the pumping of the liquid metal. The flow behaviors in the pump are very complex, including a time-varying Lorentz force and pressure pulsation, because an induction EM pump has time-varying magnetic fields and the induced convective currents that originate from the flow of the liquid metal. These phenomena lead to an instability problem in the pump arising from the changes of the generated Lorentz forces along the pump's geometry. Therefore, a magneto-hydro-dynamics (MHD) analysis is required for the design and operation of a linear induction EM pump.

We have developed a time-harmonic 2-dimensional axisymmetry MHD analysis method based on the Maxwell equations. This paper describes the analysis and numerical method for obtaining solutions for some MHD parameters in an induction EM pump. Experimental test results obtained from an induction EM pump of CLIP-150 at the STC "Sintez," D.V. Efremov Institute of Electro-physical Apparatus in St. Petersburg were used to validate the method. In addition, we investigated some characteristics of a linear induction EM pump, such as the effect of the convective current and the double supply frequency (DSF) pressure pulsation. This simple model overestimated the convective eddy current generated from the sodium flow in the pump channel; however, it had a similar tendency for the measured data of the pump performance through a comparison with the experimental data. Considering its simplicity, it could be a base model for designing an EM pump and for evaluating the MHD flow in an EM pump.

KEYWORDS : MHD Flow, EM Pump, Axisymmetry, Maxwell Equations

1. INTRODUCTION

A fast breeder reactor can utilize an electro-magnetic (EM) pump as a metal coolant pump. Since a liquid metal has an electrical conductivity, an EM pump can pump the liquid metal by the Lorentz forces in the metal flow, which result from the electrical currents ant the applied magnetic fields. Linear induction pumps especially use a traveling magnetic field wave created by poly-phase currents, and the induced currents and their associated magnetic field generate a Lorentz force whose effect can be the actual pumping of the liquid metal. [1-3]

Nowadays, small-scale EM pumps are designed easily by a simple mathematical method, and they are widely used in several industries. To pump the liquid metal in a fast breeder reactor, a large-scale EM pump can be used for a main circulation pump, which will greatly simplify a fast breeder reactor's design. However, large-scale EM pumps have some disadvantages, including pulsation of the pressure and flow instability. [1,2] Among several types of EM pumps, an annular or a cylindrical linear induction EM pump is the most promising as a large-scale EM pump in a liquid metal reactor, and some theoretical and experimental studies of these EM pumps have been carried out. [3-5] Figure 1 shows a schematic diagram of a cylindrical linear induction EM pump. The behaviors in the induction EM pump are complicated, including a time -varying magnetic field, a Lorentz force, and a pressure pulsation, because an induction EM pump works with a time-varying Lorentz force from the time-varying magnetic fields, induced currents that originate from the time-varying electric field, and convective currents following

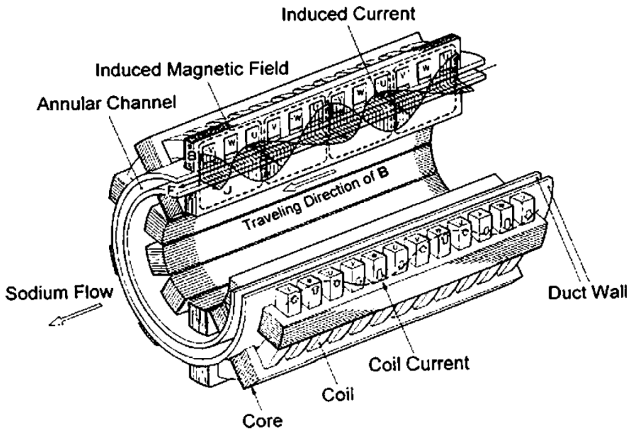

Fig. 1. Schematic Diagram of an EM Pump

the flow of the liquid metal. These phenomena might generate an instability problem in these pumps, depending on the changes of the magnetic field and the induced currents from the fluid flow of the liquid metal over time and along a pump's geometry. Therefore, a MHD analysis is required for designing a linear induction EM pump and evaluating its characteristics.

To evaluate the characteristics of a linear induction EM pump, we have developed a 2-dimensional time-harmonic stationary analysis method for an axisymmetry MHD analysis, which is based on the Maxwell equations. To validate the developed MHD analysis code, we analyzed some experimental results of a small-scale cylindrical linear induction EM pump (CLIP-150) developed and manufactured in the D.V. Efremov Institute in Russia. The CLIP-150 is a straight-through type three-phase induction pump for pumping sodium. [3] After comparing the analysis results and measured data, we found that this simple model overestimated the convective eddy current generated from the sodium flow in the pump channel. However, it had a similar tendency for the measured data of the pump performance consistent with changes in the pump conditions, such the measured current and the sodium flow. After overcoming this disadvantage, the developed model could be a base model for designing an EM pump and for evaluating the MHD flow in an EM pump.

2. DEVELOPMENT OF THE MHD ANALYSIS METHOD

We have developed a numerical method based on the Maxwell equations for MHD flow analysis in EM pumps, which consist of Faraday's Law, Ampere's Law, and Ohm's Law. [2][6] First, we developed a magnetic field analysis method based on the Maxwell equation for solving the time-varying sinusoidal magnetic field with induced currents originating from the time-varying poly-phase currents and the flow of the liquid metal. We introduced the governing equations with a magnetic vector potential to analyze the time-varying magnetic field and the Lorentz force in an EM pump. The governing equations are as follows:

$$\nabla \times \frac{1}{\mu} \nabla \times A = J \tag{1}$$

$$J = \sigma (u \times (\nabla \times A) - \frac{\partial A}{\partial t}) + J_0 \tag{2}$$

$$B = \nabla \times A \tag{3}$$

$$F_L = J \times B \tag{4}$$

where,

A = magnetic vector potential
μ = permeability
σ = conductivity
B = magnetic field
u = flow velocity
J = current density
F_L = Lorentz force

Governing equation (1) has the form of a mathematical vector curl equation. Equation (2) represents Ohm's law in a moving media with current sources, and equation (3) is the definition of a magnetic field (B) and the magnetic vector potential (A) in the magnetic field from a vector identity of the mathematics. The induced currents in equation (2) are derived as $J = \sigma(-\frac{\partial A}{\partial t})$ in the coils and $J = \sigma(u \times (\nabla \times A) - \frac{\partial A}{\partial t})$ in the sodium channel, respectively. The J_0 is the input current density in the coils from the external current sources, and it is a 3-phase sinusoidal current. The input current density can be calculated from the input current as follows: *J* = (input current)/(normal surface area). The coupling of the equations is through the Lorentz force in the momentum equation, defined as $F_L = J \times B$, where *J* is the total induced current density in the sodium channel, and the *B* is the imposed magnetic flux density ("magnetic field").

We ignored the skin effect, because the width of the sodium channel was narrow when compared with the skin depth in the applied frequency of the input voltage. [7] Generally, the width of the fluid channel in a linear induction EM pump should be limited to below the skin depth of a fluid for stable operation. The skin depth of the sodium channel in CLIP-150 was about 29.8 mm, and the width of the sodium channel was 12.4 mm, as given in the detailed pump data of Section 3. [3] Therefore, the skin effect could be negligible in this analysis, and we could eliminate the model for the skin effect of the alternating

current in the pump.

$$skin\ depth(\delta)of\ sodium = \frac{1}{\sqrt{\pi f u \sigma}} \approx 29.8mm\ \ for\ 50Hz$$

Since the CLIP-150 also had an azimuthal symmetric structure, the magnetic vector potential and induced currents could be assumed to vary only in the azimuthal direction. Accordingly, we could analyze the magnetic vector potential in an EM pump in the azimuthal direction only, allowing for a simple 2-D analysis.

In addition, we assumed the sodium velocity (u) was constant in the EM pump along the r and z directions in the sodium channel of the pump and that it was unchanged over time for a time harmonic analysis. The Hartmann number is a measure of the ratio of an electro-magnetic force to the viscous flow in an MHD flow, and the flow profile is known to become flatter when the Hartmann number becomes higher. If the Hartmann number was about 100, the flow profile was disturbed by only 5% at the near wall. [8] From the detailed data in Section 3, the Hartmann number of the CLIP-150 was about 3000. Therefore, the assumption of a uniform and constant sodium velocity seemed to be good for the MHD analysis.

$$Hartmann\ number\,(Ha) = \sqrt{\frac{\sigma B_0^2 R_0^2}{\mu_f}} \approx 3000$$

where,

σ = *electric conductivity of fluid*
B_0 = *averaged magnetic field*
R_0 = *channel width*
μ_f = *fluid viscosity*

In addition, all the time-varying parameters could be supposed to be sinusoidal because all the input currents were sinusoidal poly-phase currents. With the assumption of a constant velocity and the sinusoidal parameters, we could adopt the time harmonic assumption widely used for analyzing a general sinusoidal electromagnetic machine such as a linear machine. This assumption could eliminate the time derivatives in the equation by replacing the time derivatives in the complex term $\frac{\partial A}{\partial t} = i\omega A$. [9,10] This time harmonic analysis could dramatically reduce the computing time for a time transient analysis in a sinusoidal field, although it requires more memory to represent a complex number. Thus, the governing equation for the electro-magnetic analysis in the pump can be rewritten without the time derivative terms as follows:

$$\nabla \times \frac{1}{\mu} \nabla \times A_\theta + \sigma[i\omega A_\theta - u \times B] = J_0 \qquad (5)$$

We have developed a 2-dimensional axisymmetry numerical scheme for the above governing equation. In addition, we adopted a Coulomb gauge, $\nabla \cdot A = 0$, and an isotropic permeability. Thus, the 2-D axisymmetry curl equation was represented as follows:

$$\frac{\partial}{\partial r}[\frac{1}{\mu}\frac{1}{r}\frac{\partial}{\partial r}(rA_\theta)] + \frac{1}{\mu}\frac{\partial^2 A_\theta}{\partial^2 z} + \sigma[i\omega A_\theta - u \times B] = J_0 \qquad (6)$$

For numerical stability, we assigned a new variable; $T_\theta = rA_\theta$ and rewrote the vector potential equation. [11] We derived a finite difference method (FDM) for solving the above modified vector potential equation. [9,10,12] In an EM pump, various interfaces existed between the stators, the coils, the steel ducts, the air gaps and the sodium channel. We derived the interface scheme to assign the material properties and current sources at the interfaces in the FDM code. Figure 2 shows the general interface in the problem domain. In the FDM, the interface considered the eddy current area analyzed by a five-point scheme. The parameters in each cell could be different. The above equation could be rewritten in the form of a curl.

$$\nabla \times (1_z \frac{1}{\mu}\frac{1}{r}\frac{\partial T_\theta}{\partial r} - 1_r \frac{1}{\mu}\frac{1}{r}\frac{\partial T_\theta}{\partial z}) = J_o - i\sigma\omega\frac{T_\theta}{r} + \sigma[u \times B] \qquad (7)$$

Integrating both sides of the above equation over the domain bounded by 1,2,3, and 4 and making use of Stokes' theorem in the left-hand side, [9][10] we could obtain

$$\int_{1234} \nabla \times (1_z \frac{1}{\mu}\frac{1}{r}\frac{\partial T_\theta}{\partial r} - 1_r \frac{1}{\mu}\frac{1}{r}\frac{\partial T_\theta}{\partial z}) \bullet 1_l dl = \int_1^2\int_3^4 (J_o - i\sigma\omega\frac{T_\theta}{r} + \sigma[u \times B])dS \qquad (8)$$

The analysis of all the particular contributions to the line integrals leads to a formula expressing the value of T_θ at the central point 0 by the surrounding nodes in the FDM formulation, as shown in Fig. 2.

$$\alpha_1(T_1 - T_0) + \alpha_2(T_2 - T_0) + \alpha_3(T_3 - T_0) + \alpha_4(T_4 - T_0) = -J_0 + Q_0 T_0 - B_0 \qquad (9)$$

where,

$$\alpha_1 = [h_2/\mu_1 + h_4/\mu_4]/2h_1/r_0$$

$$\alpha_2 = [h_1/\mu_1 + h_3/\mu_2]/2h_2/(r_0 + h_2/2)$$

$$\alpha_3 = [h_2/\mu_2 + h_4/\mu_3]/2h_1/r_0$$

$$\alpha_4 = [h_1/\mu_4 + h_3/\mu_3]/2h_2/(r_0 - h_4/2)$$

$$\sigma_0 = \frac{h_1}{2}\frac{h_2}{2}\sigma_1 + \frac{h_2}{2}\frac{h_3}{2}\sigma_2 + \frac{h_3}{2}\frac{h_4}{2}\sigma_3 + \frac{h_4}{2}\frac{h_1}{2}\sigma_4$$

$$J_0 = \frac{h_1}{2}\frac{h_2}{2}J_1 + \frac{h_2}{2}\frac{h_3}{2}J_2 + \frac{h_3}{2}\frac{h_4}{2}J_3 + \frac{h_4}{2}\frac{h_1}{2}J_4$$

$$Q_0 = i\omega\sigma_0/r_0$$

$$B_0 = \sigma_0 u \times B$$

Since $B_r = \frac{1}{r_0}\cdot(T_1 - T_3)/(h_1 + h_3)$ and u were assumed to be constant of u_z in only the z direction along the (r, z) directions, the coefficient α_1, α_3 with the sodium flow in the channel could be represented as follows:

$$\alpha_1 = \alpha_1 - u_z \cdot \frac{1}{r_0}\sigma_0/(h_1 + h_3)$$
$$\alpha_3 = \alpha_3 + u_z \cdot \frac{1}{r_0}\sigma_0/(h_1 + h_3) \quad (10)$$

In the magnetic vector potential equation, the external supply input currents, as well as the induced currents and the convective current originating from the flow of the electrically conductive metal, acted as a source of the magnetic field in the EM pump. The supply current and sodium flow rate were given as input data. The boundary conditions of the magnetic vector potential (A_θ) were all zero.

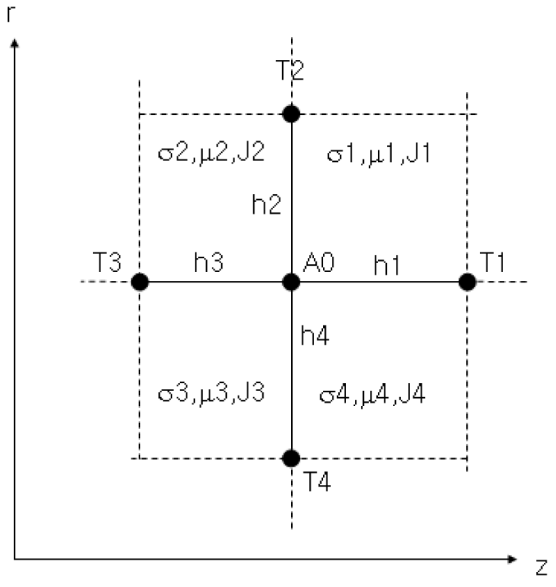

Fig. 2. Discretization of the Problem Domain

3. SPECIFICATIONS OF THE CLIP-150 EM PUMP

The CLIP-150 was developed, manufactured and tested at the D.V. Efremov Institute (NIIEFA) in Russia. The pump was designed and manufactured as an experimental model for a detailed study of EM pump characteristics. [3] The CLIP-150 was tested in a liquid metal facility, consisting of a liquid metal loop, a system for filling the loop with sodium, an electrical heating system, and other components. The pump's flow rate was 0.5~2.9m^3/min, and it was a kind of 50 Hz three-phase induction EM pump with a cylindrical linear duct intended for pumping sodium. In addition, it was a straight-type pump. The pump consisted of the following main components: inductors (outer stators) with excitation windings, a straight-through duct, and an inner magnetic core. The pump inductor consisted of magnetic core blocks assembled from stamped electrical-sheet steel. The excitation winding, consisted of 36 disc coils made of copper wire. The pump duct was of a straight-type and consisted of two coaxial pipes made of stainless steel. The structure of the CLIP-150 is shown in Fig. 3, and its main specifications are shown in Table 1. The tests were carried out on sodium at a sodium temperature of 300 $\pm$5°*C*. The temperature was kept constant during the tests and the flow rate was controlled by a control valve. Three-phase electric power was supplied to the CLIP-150 during the tests from a 50 Hz autotransformer. Voltages, currents, and consumed powers in CLIP-150 were measured, and the sodium pressures at the inlet and outlet were measured.

Table 1. Main Specifications of the CLIP-150

Flow rate	0.5~2.9 m^3/min
Developed pressure	0.11~0.44 MPa
Frequency	50 Hz
Phase	3
Phase connection	star Y
No. of poles	6
Input power	4.08x10^4 W
No. of slots	36
EMP height	0.1745 m
Stator length	0.908 m
Stator height	0.114 m
Core height	0.031 m
Permeability of sodium	1 (relative)
Electrical Conductivity of sodium (at 300 °C)	5.7x10^6 S/m
Temperature of sodium	300 °C
Density of Na (at 300 °C)	880 Kg/m^3
Kinematic Viscosity of Na (at 300 °C)	3.9x10^{-7} m^2/sec

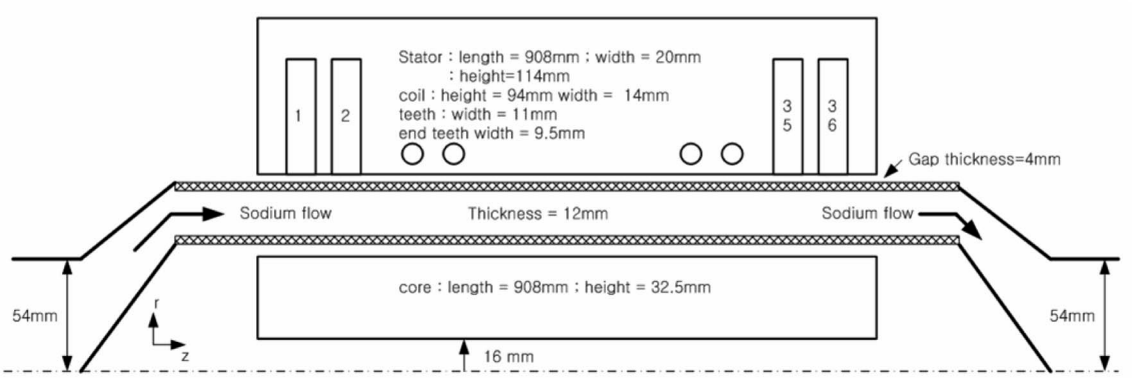

Fig. 3. Structure of the CLIP-150

4. ANALYSIS RESULTS

4.1 Analysis Domain

To analyze the characteristics of the CLIP-150, we selected the analysis domain shown in Fig. 4 and the source coils in Fig. 5. As shown in Figs. 4 and 5, the analysis domain consisted of various materials, suck as stators, coils, air gaps, steel duct walls, and the sodium channel. We assigned a material property for each region. Then, we analyzed the MHD flow in the CLIP-150, where a total non-equidistant computational mesh of 52(r) $\times$330(z) control volumes was used. The control volumes in the sodium region were composed of 10(r) $\times$330(z) volumes, the outer stator was divided into 20(r) $\times$186(z) volumes, and the inner core was divided into 10(r) $\times$290(z) volumes, while slot was made of 10(r) $\times$4(z) control volumes. Additionally, the air gap region at both ends of CLIP-150 was divided by 10(r) $\times$ 20(z) volumes.

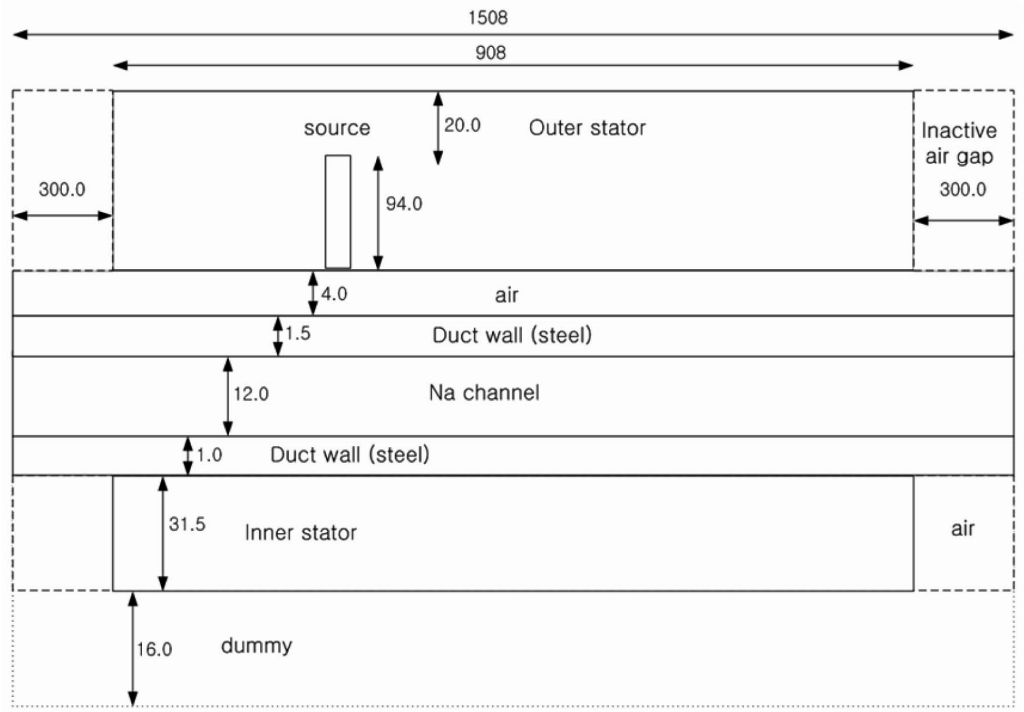

Fig. 4. Analysis Domain for the CLIP-150 (unit: mm)

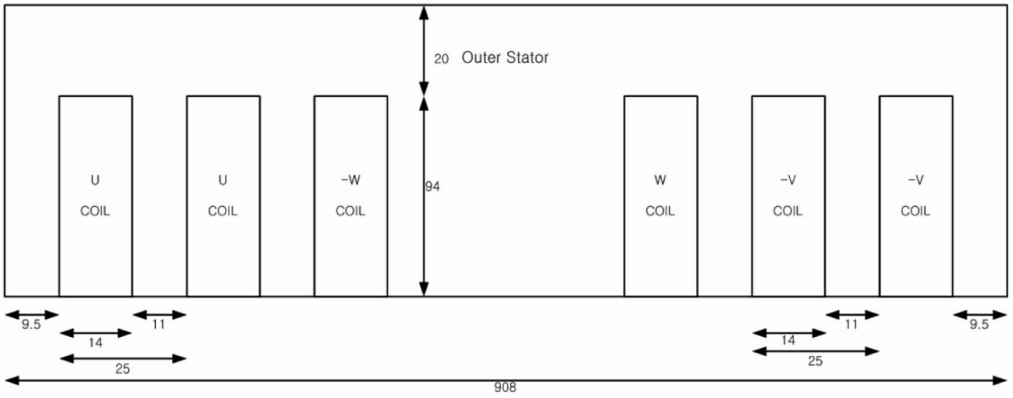

Fig. 5. Source Coils for the CLIP-150 (unit: mm)

4.2 Characteristics Between the Developed Pressure and the Flow Rate

With the developed code and measured input currents, we analyzed the time-harmonic characteristics of the CLIP-150 and verified the developed code with experimental data. The time-averaged Lorentz force, which was a body force for the EM pump during cycle duration, was defined as follows.

$$F_{Lorentz} = -\frac{1}{2}\mathrm{Re}\{B \times J^*\} \tag{11}$$

where

B = *magnetic field*

J^* = *Conjugate complex of the induced currents*

Since we focused on the Lorentz force along the z direction in the frequency domain, the body force could be rearranged as follows, where F_z refers to the Lorentz force in the z direction:

$$\begin{aligned} F_z &= -\frac{1}{2}\mathrm{Re}\{B_r \cdot J_\theta^*\} \\ J_\theta &= \sigma(-i\omega A_\theta + u_z \cdot B_r) \end{aligned} \tag{12}$$

In addition, the developed pressure through the EM pump could be defined as follows.

$$\Delta P_{developed} = \frac{1}{S}\int_{S\times L} F_z dS dl = \frac{1}{S}\sum F_z^i dS^i dl^i \tag{13}$$

We analyzed the developed pressure of the CLIP-150 with the measured input currents and sodium flow rates (sodium velocities). The results of the analysis and the measured data are shown in Fig. 6. From this result, we found relationships between some MHD parameters. The applied magnetic field in the sodium channel was proportional to the input currents, while the developed pressure was proportional to the square of input current but inversely proportional to the velocity of sodium flow.

The results showed that the developed pressure of the analysis results underestimated the measured developed pressure, although the trends of the analysis results followed the experiment results well. The reason for the discrepancy is thought to be that the model overestimated the convective eddy current term [$J_e = \sigma[-u \times B]$]. In order to overcome this problem, we think that some constraints

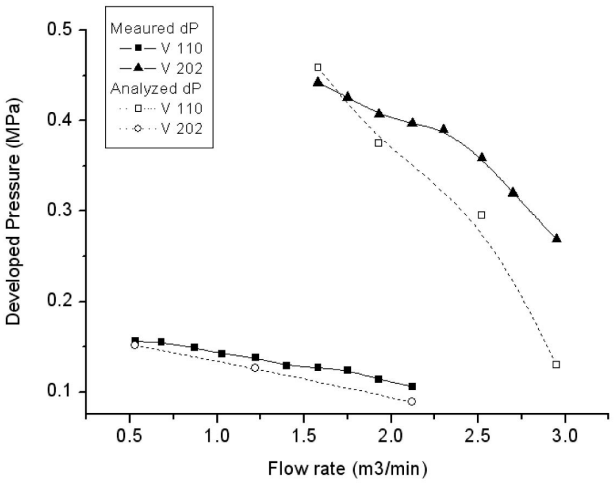

Fig. 6. Developed Pressure and Flow Rate with the Input Voltages

are needed, such as the continuity of a current, for an exact analysis of the convective eddy current. We will study this matter later.

However, the model seems to have a good tendency that can represent the characteristics presented in Section 4.3. Although the convective term in this model was overestimated, its effect on the MHD parameters of the EM pump, except for the developed pressure, could be negligible, as shown in Section 4.3.

4.3 Characteristics of the Magnetic Fields and the Induced Currents in the Sodium Channel

In this paper, we evaluated the effect of a change of the sodium flow and input currents in the CLIP-150 among the various characteristics of the EM pump. The major difference between an EM pump and a mechanical pump is that the fluid is pumped by the Lorentz force without an impeller in an EM pump. The Lorentz force is generated by the eddy current and the applied magnetic field in the sodium channel of the EM pump. The applied magnetic field is produced by the input currents and the eddy current in the channel. The eddy current in the channel consists of the time derivative term generated by the time-varying magnetic field and the convective term originating from the sodium flow. The Lorentz force by the time derivate term propels the sodium, but the Lorentz force by the convective term repels the flow in the pump channel. In addition, the eddy current can distort the applied magnetic field in the channel by the input currents, and the convective term can be a dominant cause for an end effect. An end effect means that strong repulsion forces occur at both stator ends of the EM pump. This end effect is a major cause of a DSF pressure pulsation, because the magnitude of an end effect varies over time. The DSF pulsation is one of the most important problems in the operation of an EM pump. Therefore, we examined a change of the magnetic field and the eddy current density in the sodium channel resulting from a change of the sodium flow rate and the applied current to the EM pump among various characteristics of the EM pump.

From the analysis results, we investigated the magnetic field and the induced eddy currents in the sodium channel in the CLIP-150. In the case of a 202 V input voltage and a 1.58 m^3/min flow rate (u=6.45m/sec), the magnetic field, induced current, and Lorentz force along the longitudinal (z) direction and the radial (r) direction in the sodium channel are shown in Fig. 7. The Lorentz force along the radial direction was less than 1/10 times that of the longitudinal direction. Therefore, the CLIP-150 could pump the sodium along the longitudinal direction without consideration of pressure dispersion in the radial direction, so we only analyzed Lorentz force for CLIP-150 in the z direction for analyzing the developed pressure. All the variables were time-averaged values during a frequency cycle. Since we introduced a stationary analysis tool in the frequency domain, we could analyze the time-averaged results during a frequency cycle. By investigating the Lorentz force along the z direction, we could elucidate the end effect of the CLIP-150. The Lorentz forces due to the sodium flow were shown as a strong repulsive force at both ends of the EM pump, with a magnitude at the outlet that was larger than that at the inlet. Since the CLIP-150 is a kind of linear induction machine, it must have an end effect due to a cutting of the magnetic fields with the convective eddy currents at both ends of the EM pump.

Next, we examined the effect of a change of the sodium flow in the CLIP-150. The convective eddy current from the sodium flow can distort the applied magnetic field and the magnetic vector potential. Therefore, we evaluated the magnitude of a distortion of the magnetic field and the Lorentz force in the radial direction according to the sodium flow. We found that the distortion from a change of the convective eddy current by the sodium flow and the Lorentz force in the radial direction was negligible.

In the case of the 202 V input voltage with flow rates of 1.58 m^3/min (u=6.45m/sec) and 2.95 m^3/min (u =12m/sec), we examined a change of the MHD parameters of the CLIP-150 with various flow rates. Since the real and imaginary part of the electro-magnetic variables in the CLIP-150 had a nearly similar magnitude, as shown in Fig. 7, we only examined the real part of the variables with various flow rates of the CLIP-150. Figure 8 shows the MHD parameters of the sodium channel in the CLIP-150 with various flow rates. The magnetic vector potential, longitudinal Bz field, and radial Br field were slightly increased by the flow rates. However, the effect due to a change of the flow rate was negligible, as shown in Figs. 8 (a)-(c). The induced current was composed of a time-varying part (frequency part in this analysis) and a convective part due to the sodium flow. The time-averaged value of the time-varying part of the induced current can be represented by $J = -\sigma \frac{\partial A}{\partial t} = -i\sigma\omega A$, and it was slightly changed due to a slight change of the magnetic vector potentials according to the various flow rates. The convective part of the induced currents was represented as $J = \sigma(U \times B) = \sigma(U_z \cdot B_r)$, and it was proportional to the flow rate, as shown in the definition. Finally, the Lorentz forces were changed by the flow rate, because the convective term of the induced currents was highly dependent on the flow rate. The Lorentz force of $F = -i\sigma\omega A \cdot Br$, which originated from the time-varying magnetic field, was slightly changed due to an increase of the magnetic vector potential and the magnetic field, according to a change of the flow rate in the CLIP-150. On the contrary, the Lorentz force of the convective term ($F = \sigma(U_z \cdot B_r) \cdot B_r$) was strongly dependent on the flow rate. This term of the Lorentz force was in an opposite direction to the applied magnetic fields, and it generated an end effect at both ends of the EM pump. Otherwise, the repulsive forces, which counteracted an abrupt change

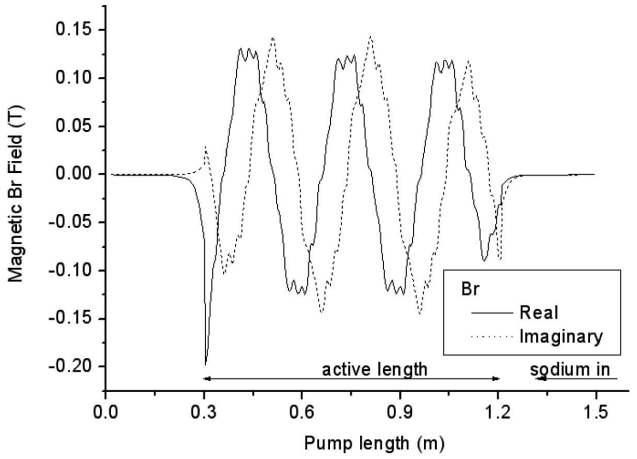

(a) Radial magnetic field

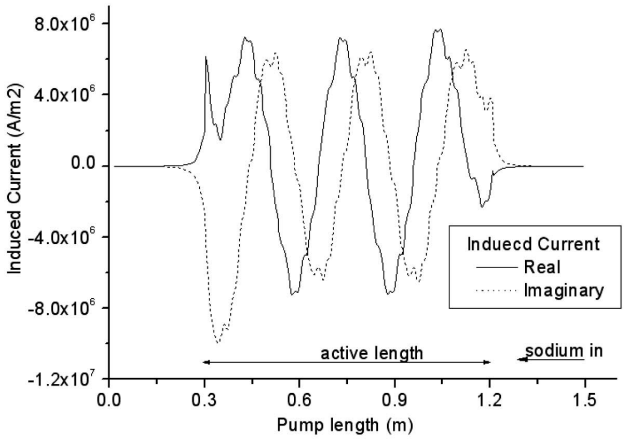

(b) Induced currents

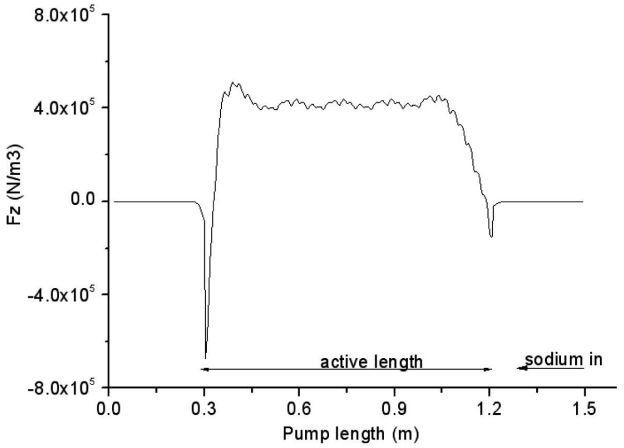

(c) Lorentz force in the longitudinal direction

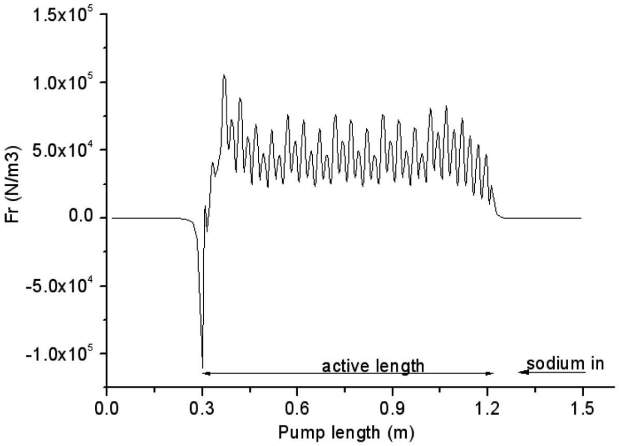

(d) Lorentz force in the radial direction

Fig. 7. MHD Parameters in the Sodium Channel

of the magnetic fields with the convective eddy currents, were produced at both ends of the stator in the EM pump. The magnitude of the repulsive Lorentz forces and the end effects were strongly proportional to the flow rate. When the sodium flow was zero, the term of the repulsive forces at both ends disappeared, as shown in Figs. 8 (e)-(g). The magnitude of the end effect was larger at the outlet of the EM pump. Therefore, the required power for the EM pump should be increased monotonically by the flow rate to overcome the repulsive Lorentz force and end effect.

4.4 Time Transient Analysis

First, we analyzed the MHD flow in the EM pump in the frequency domain with the developed code. In order to examine the time transient behavior, such as pressure pulsation, we transformed the analysis results from the frequency domain into the time domain. The time transient behavior from a general function in the frequency domain could be obtained by the following equation.

$$\phi(r,z)\exp(i\omega t+\theta)=\mathrm{Re}[\phi^{0}(r,z)\{\cos(\omega t+\theta)+i\sin(\omega t+\theta)\}]$$
$$=\phi^{0}(r,z)\cos(\omega t+\theta) \quad (14)$$

where,

$$\phi^{0}=\sqrt{\phi_{real}(r,z)^{2}+\phi_{imaginary}(r,z)^{2}}\,,$$

$$\theta=\mathrm{sgn}\{\arctan(\frac{\phi_{imaginary}}{\phi_{real}})\}\,.$$

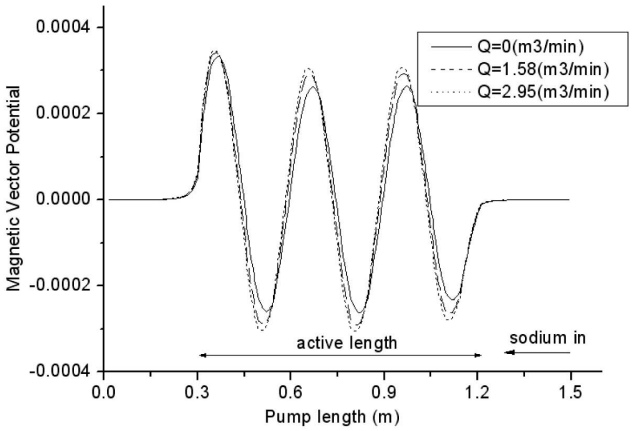

(a) Magnetic vector potential with various flow rates

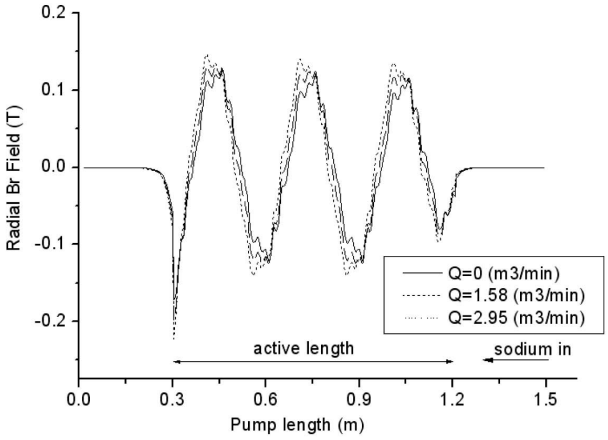

(c) Radial magnetic field with various flow rates

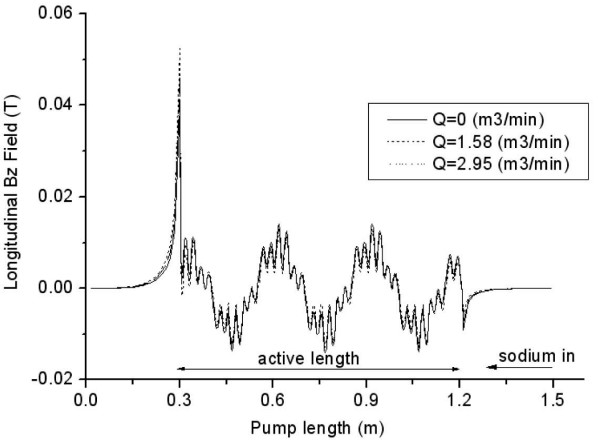

(b) Longitudinal magnetic field with various flow rates

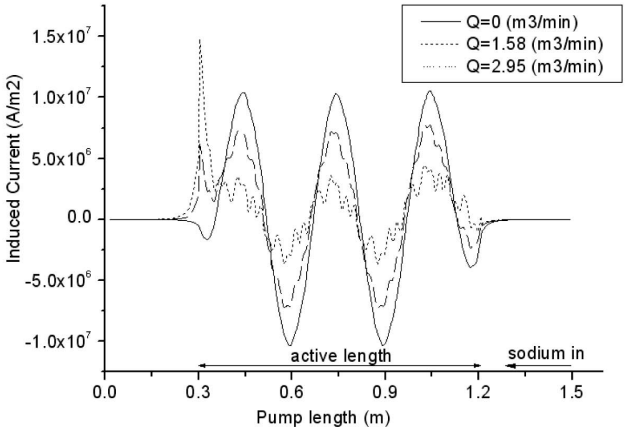

(d) Induced eddy current with various flow rates

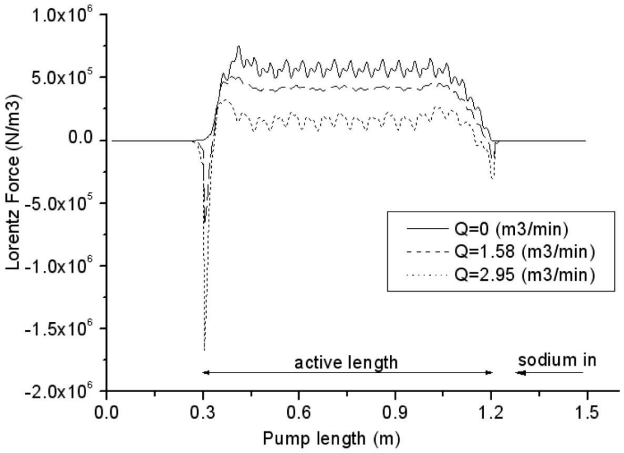

(e) Lorentz force with various flow rates

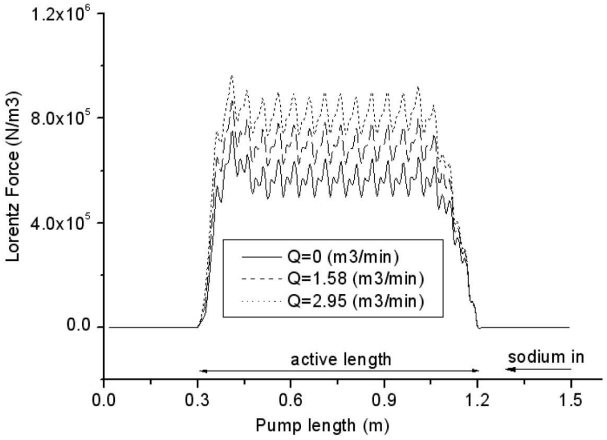

(f) Lorentz force by the eddy current from time-varying potentials with various flow rates

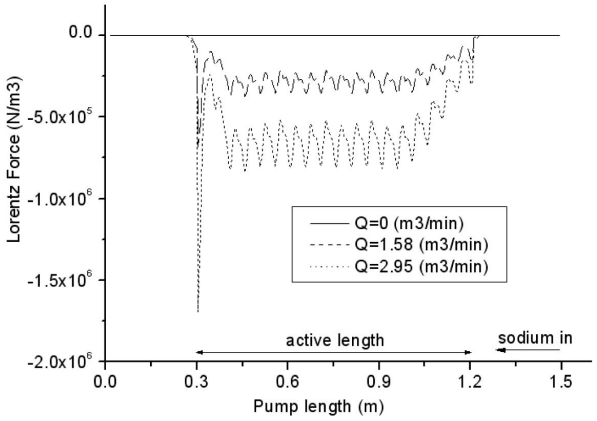

(g) Lorentz force by the convective eddy current with various flow rates

Fig. 8. MHD Parameters with Various Flow Rates

The sign of θ was determined by the location of ($\phi_{imaginary}$, ϕ_{real}) in the quadrant. Therefore, the time transient behavior of each electro-magnetic variable was as follows.

$$B_r(r,z,t) == B_r^0(r,z)\cos(\omega t + \theta_1) \tag{15}$$

$$J_\theta(r,z,t) == J_\theta^0(r,z)\cos(\omega t + \theta_2) \tag{16}$$

Then,

$$F_z(r,z,t) = F_z^0(r,z)\cos(2\omega t + \theta_1 + \theta_2)\,. \tag{17}$$

From the above equations, we could deduce the DSF pressure pulsation. [1, 5] We analyzed the time transient behavior with the DSF pressure pulsation in the case of a 202 V input voltage and a flow rate of 1.93 m^3/min. Figure 9 shows the time transient magnetic flux density, the induced current, and the Lorentz force in this case. From the analysis results in Fig. 9 (c), we found that the pulsation of the Lorentz force could be nearly averaged through the active core region along the z direction during a frequency cycle, and the sign of the magnitude was always positive. At both ends of the active core region in the EM pump, the magnitude of the integral Lorentz force was changed over time. Figure 10 shows the integral Lorentz forces over time. Therefore, we concluded that the magnitude of the DSF pressure pulsation was dominantly affected by the end effect. The magnetic field and the induced current oscillated with the input frequency of 50 Hz (cycle duration=0.02sec), and the Lorentz force oscillated

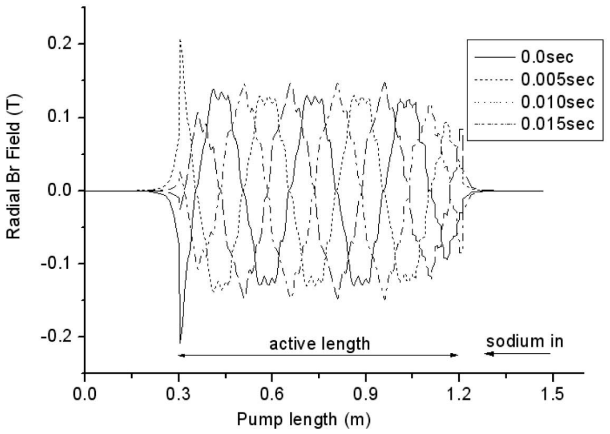

(a) Radial magnetic field over time

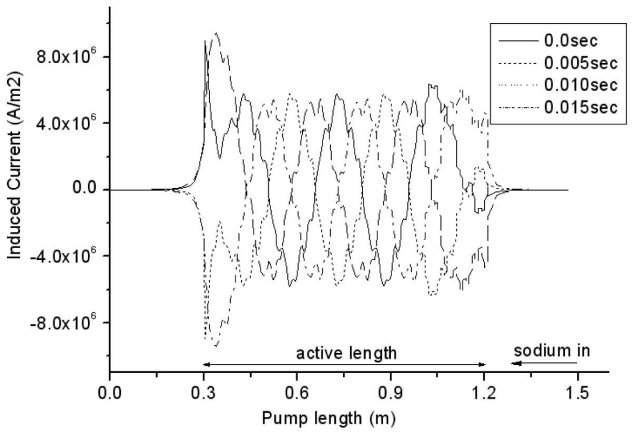

(b) Induced current over time

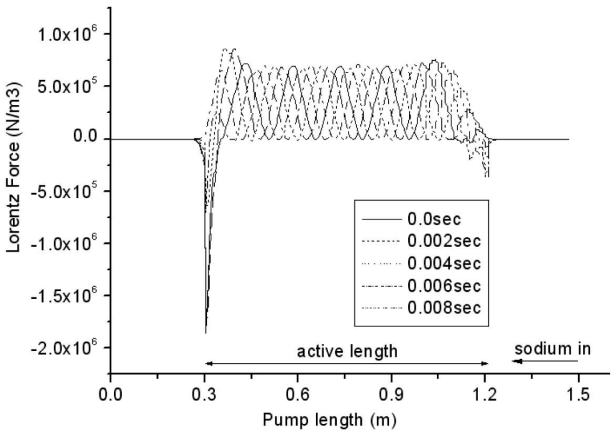

(c) Lorentz force over time

Fig. 9. MHD Parameters Over Time

with a double frequency of the input frequency as mentioned above and as shown in Fig. 10. Otherwise, the integral magnitude of the Lorentz force was nearly in an equilibrium

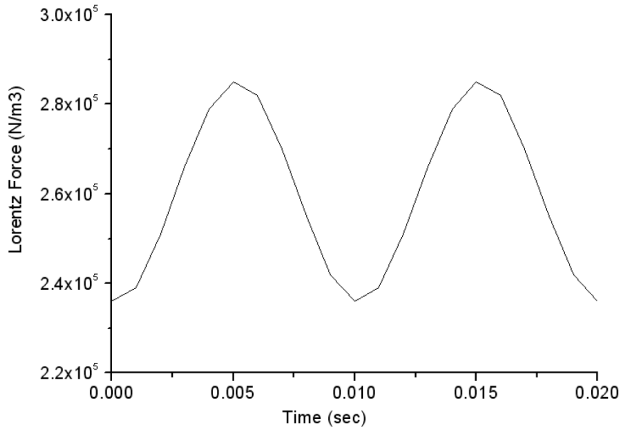

Fig. 10. Integral Lorentz Force Over Time

state in the active core region, and the magnitude at both ends oscillated at two times (double) that of the frequency of the input voltages. Finally, the integral Lorentz force oscillated with a double frequency supply of the input voltage over time, which is called a DSF pressure pulsation.

We found that the magnitude of the DSF was nearly proportional to the flow rate, because the magnitude of an oscillation at both ends increased monotonically with the flow rate. The relative magnitudes of the DSF pressure pulsations with various flow rates are shown in Fig. 11 for the case of a 202 V input voltage. This could suggest a method for minimizing the DSF pressure pulsation of an EM pump, such as linear grading of the input coils.

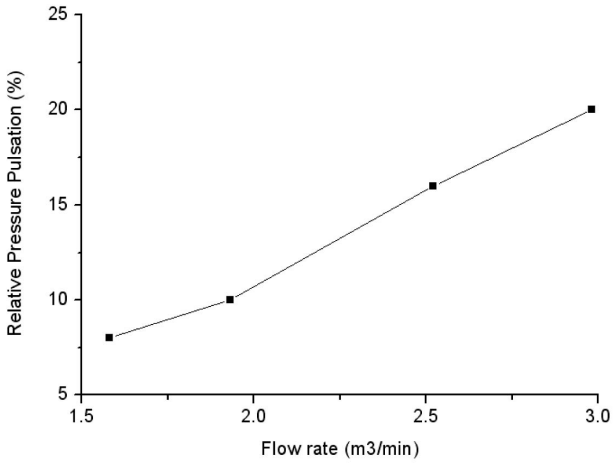

Fig. 11. Relative DSF Pressure Pulsation with the Flow Rates

5. CONCLUSIONS

We have developed a 2-D axisymmetry time-harmonic MHD analysis method in the frequency domain for a linear induction EM pump by using sinusoidal inputs and electro-magnetic fields, and the results could be easily transformed into the time domain. We verified the analysis method through a comparison with the experimental data of a CLIP-150 EM pump, which was designed and manufactured at the D.V. Efremov Institute in Russia. We used the measured currents as sources instead of the applied voltages for the analyses and assumed a constant velocity of the sodium for analyzing a stationary field of the CLIP-150. We investigated the characteristics of the MHD flow in a linear induction EM pump with the developed analysis method.

The analysis results slightly underestimated the developed pressure with the applied input currents. The reason is that the method has a tendency to overestimate the convective eddy current generated from the sodium flow. This can be overcome by adopting a constraint for the current continuity in the sodium channel when calculating the term of the convective eddy current. In addition, we will use the applied input voltages for the input power sources instead of the input currents and develop a 3-dimensional time transient MHD code. This will allow us to analyze the physical phenomena of the EM pump more accurately and in more detail and to evaluate an instability problem for a large EM pump, such as a low frequency pressure pulsation as well as a DSF pressure pulsation.

ACKNOWLEDGEMENTS

This study has been carried out under the Nuclear R&D Program supported by the Ministry of Science and Technology, Republic of Korea.

REFERENCES

[1] Araseki, H., et al, "Double-supply-frequency pressure pulsation in annular linear induction pump Part I: Measurement and numerical analysis," Nuclear Engineering and Design, Vol. 195, 85 (2000).

[2] Baker, R.S. and Tessier, M.J, 1987, Handbook of Electromagnetic Pump Technology, Elsevier Science Publishing Co., Inc. (1987).

[3] Kirillov, I.R. and Ogorodnikov, A.P., Test Results of CLIP-3 /150, Sintez D.V.Efremov Institute in Russia (2000).

[4] Kirillov I.R. and Obukhov D.M., "Two-dimensional model for analysis of cylindrical linear induction pump characteristics: model description and numerical analysis," Energy conversion and management, Vol. 44, 2687 (2003).

[5] Kirillov I.R., et al, "Comparison of computer codes for evaluation of double-supply-frequency pulsations in linear induction pumps," Nuclear Engineering and Design, Vol. 231, 177 (2004).

[6] S.A. Nasar, I. Boldea and TR. Vuia, Linear Motion Electric Machines, Johns&Sons (1976).

[7] Matthew N.O. Sadiku, Elements of Electromagnetics, Oxford

University Press (2001).
[8] Hong S.H. et al, Development of LMR Coolant Technology – Development of Submersible-In-Pool Electromagnetic Pump, KAERI/CM-089/96 (1996).
[9] Andrzej K. and Tegopoulos J.A., Numerical Modeling of Eddy Currents, Clarendon Press. Oxford (1993).
[10] EKriezis E.E., et al, "Eddy currents: Theory and Applications," Proceedings of the IEEE, Vol. 80, No.10, 1599 (1992)
[11] Nakata T., "Finite element analysis of magnetic circuits composed of axisymmetric and rectangular regions," IEEE trans. on Magnetics, Vol. Mag-21, No.6, 2199 (1985)
[12] Binns, K.J., Lawrenson P.J. and Trowbridge C.W., The Analytic and Numerical Solution of Electric and Magnetic Fields. Johns&Sons (1992).